

## **Bicycle Helmet Retention Strength Test Procedures Comparison**

**Edward B. Becker**  
**Snell Memorial Foundation**  
**December 3, 1998**

### **Abstract**

The tests for the dynamic strength of bicycle helmet retention systems as prescribed in the Consumer Product Safety Commission Bicycle Helmet Safety Standard and as previously described in the Snell Memorial Foundation 1995 Standard for Protective Headgear for Use in Bicycling were compared in tests of real and simulated bicycle helmets. The Snell procedures apply 20% to 25% higher levels of force but, in actual helmet testing, the CPSC procedures measure slightly greater elongation.

### **Introduction**

Many of the currently followed helmet standards require that the retention systems yield no more than a certain amount of stretch under a prescribed shock loading. A platform is suspended from the buckled chinstrap and a mass is dropped onto it from a prescribed height. The shock of the impact is transferred directly to the chinstrap, its closure and its attachments to the helmet. If stretch or mechanical failure allow the platform to descend more than a certain distance, the helmet will be rejected.

Although the standards have generally agreed on the description of the upper end of the platform which rests directly on the chinstrap and which simulates the bones of the wearer's jaw, the masses, drop distances and other parameters have varied widely. For example: the Snell test as prescribed for the B-95 bicycle helmet standard and shown in figure 1 called for a 38 kilogram shock mass to be dropped through a distance of 30 mm while the current CPSC test shown in figure 2 calls for 4 kg to be dropped through 600 mm. The Snell shock mass is 9.5 times greater than CPSC's but the CPSC drop height is 20 times greater than Snell's suggesting a test more than twice as severe overall.

Since the Snell B-95 test had been based on measures of plastic buckle strengths and the performance of the most commonly encountered bicycle helmet retention systems, a test more than twice as severe could reasonably be expected to produce many failures. However, most laboratories found that there was no increase in the failure rate. In order to substantiate this finding, the Snell laboratory in North Highlands, California, performed CPSC and B-95 type tests upon samples of similar helmets and upon a helmet retention system composed of cot springs which approximated the force response behavior of the chinstraps of most commercially available bicycle headgear.

### **Method**

The lab acquired four samples each of five different bicycle helmet configurations. Two of each configuration were tested for retention strength according to Snell B-95 and two were tested according to CPSC for a total of ten helmet tests for each procedure. All twenty samples were in brand-new condition prior to testing. Since the results of the second and third tests on a sample differ greatly from the first result, this study considers only the results of the first retention strength test performed on these samples.

Platform displacement was measured with a potentiometer while force measurements were taken from a transducer mounted just beneath the simulated jaw. The data was collected dynamically allowing detailed comparison of the force versus displacement response of the various helmets.

Since only a single set of results could be obtained from any helmet sample, results were also collected for a simulated helmet retention system. This simulation substituted short lengths of steel channel for the headform and simulated jaw shown in figures 1 and 2. These lengths of channel were connected by four cot springs selected such that the springs permitted up to forty millimeters of peak elongation and would produce a peak force of up to 300 lbs.

This assembly reproduced the elastic portion of the loading curve noted for the bicycle helmet retention systems reliably and reproducibly. It did not reproduce the non-elastic behavior noted at the beginning of the CPSC response nor the behavior noted for both procedures after the retention system reached peak displacement. Even so, the simulation seems a useful means for comparing the Snell and CPSC test procedures.

### Results and Analysis

Samples of the results for a B-95 test are shown in figures 3 through 5, and for CPSC in figures 6 through 8. The results of the helmet tests are summarized in the following table:

Table 1. Helmet Test Results

	CPSC			Snell B-95		
	Disp mm	Force lbs	Work Joules	Disp mm	Force lbs	Work Joules
Average	26.7	201.9	13.0	24.9	264.1	17.8
Deviation	1.4	16.4	0.50	1.4	11.0	0.54

The differences in helmet configuration seemed to have no effect on performance. The peak displacements and forces were remarkably repeatable for both the Snell and CPSC tests. However, there were differences for the two different procedures. The CPSC peak displacement measures averaged 7% more than Snell while the Snell peak force measures averaged 23% more than CPSC. Work is based on an integration of the force and displacement measures and will be explained more fully below. These differences in peak force and displacement were statistically significant but, remarkably, give contrary indications about the relative severity of the two procedures.

Much of the force versus displacement behavior of a bicycle helmet retention system is determined by the strapping material. Since the two series of tests involved identical sets of helmets, the loading portions of the cross-plots of force versus displacement should be similar. Figure 9 shows the force versus displacement curves obtained in the Snell testing and figure 10 shows the same response for the CPSC tests. Figure 11 shows the CPSC data superimposed on the Snell data and displacement shifted to obtain the best alignment for the loading portions of the curves. Essentially, the loading behavior identifies corresponding baselines for the Snell and CPSC tests and suggests that the Snell zero displacement position is the same as the CPSC 7 mm

displacement position. If the 7 mm is added in to the Snell peak displacement average, then the Snell peak displacement and peak force both are about 20% greater than the corresponding CPSC peak values. Both measures now agree and indicate that the Snell test is about 20% more severe than the CPSC test, at least in terms of system stress.

Since both tests limit the maximum displacement allowed to 30 mm, the CPSC test is more difficult. Snell imposes more stress but, including the 7 mm shift figure, allows about 20% more displacement. If a helmet is prone to buckle, strap or rivet failure, Snell B-95 will fail it first but if component failure is not an issue, then the CPSC test is more demanding. However unlikely, it is hypothetically possible for a helmet to pass either one of these tests and fail the other.

This 7 mm shift is due to the fact that the Snell apparatus preloads the retention system with 24 kg. Practically all of this preload is in a weight that rests on a second platform on the chinstrap loading assembly. When the 38 kg shock load strikes the main platform, the assembly is yanked out from under the preload which is caught by a set of stops effectively removing it from further interaction. Since the chinstrap is under about 26 lbs of tension before the test begins, there is no residual looseness in the system. The chinstrap is already in the domain of elastic response. The CPSC preload is limited to the 7 kg mass of the platform apparatus. Although this load implies as much as 8 lbs of tension in the chinstrap prior to the shock, there appears to be as much as 7 mm of looseness that must be drawn out of the chinstrap before it begins to respond elastically to further displacement.

This explains the seeming contradiction between the peak force and peak displacement observations for Snell and CPSC. However, just how the Snell test produces greater forces and real displacements remains to be answered.

When the mass strikes the platform, there are two governing principles, momentum must be conserved, and the kinetic energy must not increase.

$$m_i u_i + m_p u_p = m_i v_i + m_p v_p$$
$$\frac{1}{2} m_i u_i^2 + \frac{1}{2} m_p u_p^2 \geq \frac{1}{2} m_i v_i^2 + \frac{1}{2} m_p v_p^2$$

where:

$m_i, m_p$  are mass values for the impact mass and platform

$u_i, u_p$  are the initial velocities of the impact mass and platform mass

$v_i, v_p$  are the velocities immediately afterward

Expressions for the velocities immediately after impact can be written in terms of a coefficient of restitution.

The energies

$$v_i = \frac{m_i - e m_p}{m_i + m_p} u_i + \frac{m_p(1+e)}{m_i + m_p} u_p = \frac{1-e\alpha}{1+\alpha} u_i + \frac{\alpha(1+e)}{1+\alpha} u_p$$

$$v_p = \frac{m_i(1+e)}{m_i + m_p} u_i + \frac{m_p - e m_i}{m_i + m_p} u_p = \frac{1+e}{1+\alpha} u_i + \frac{\alpha-e}{1+\alpha} u_p$$

where:

$$e = \text{coefficient of restitution} = \frac{v_p - v_i}{u_i - u_p} \quad \text{and} \quad 0 \leq e \leq 1$$

$$\alpha = \frac{m_p}{m_i}$$

immediately before and after the first impact are:

$$E_o = \frac{1}{2} m_i v_o^2$$

$$E_i = \left( \frac{1-e\alpha}{1+\alpha} \right)^2 E_o$$

$$E_p = \alpha \left( \frac{1+e}{1+\alpha} \right)^2 E_o$$

The coefficient of restitution depends on the materials, shapes and orientations of the impacting bodies. The value of this coefficient for steel spheres in impact is often approximated as 5/9. This is the value used in the following development but actual values will generally be lower and will depend on local implementation of the procedures. The table below shows the various mass and preload parameters for the two sets of procedures.

Table 2. Test Equipment Parameters

	Drop Height	Impact Mass	Platform Mass	Preload Mass
B-95	30 mm	38 kg	2 kg	24 kg
CPSC	600 mm	4 kg	7 kg	7 kg

The theoretical energies and velocities become:

Table 3. CPSC Impact Interaction

CPSC	Impact Mass		Platform Mass	
	Velocity	Energy	Velocity	Energy
Before	3.43 m/s	23.5 J	0	0
After	0.03 m/s	0.0 J	1.94 m/s	13.2 J

Table 4. B-95 Impact Interaction

B-95	Impact Mass		Platform Mass	
	Velocity	Energy	Velocity	Energy
Before	0.77 m/s	11.2 J	0	0
After	0.71 m/s	9.5 J	1.13 m/s	1.3 J

It is immediately obvious that the impact transfers far less energy for the B-95 procedures than for CPSC. However, after the impact, the velocity of the CPSC impact mass is essentially zero. Although the CPSC impact mass is still under the influence of gravity, it will not make a second contact with platform until well after the platform has reached its maximum deflection and is on the way back up. This second impact may be seen directly in figure 7 as the small peak at just past 50 milliseconds.

The B-95 impact mass velocity after impact is still more than 90% of its initial value. Although the velocity of the platform mass is 60% greater, the platform will slow rapidly due to the pre-tensioning of the chinstraps by the preload mass. The impact mass will quickly overtake the platform and strike it again and again transferring more energy and, finally, matching velocities with it so that platform and impact mass move together as a unit. Evidence of this progression of impacts is present as the series of spikes at the beginning of the force versus time plot in figure 4.

The conditions for subsequent impacts in the B-95 test can be approximated by postulating that the average velocity for the platform and impactor between impacts must be the same. If we ignore the acceleration of the impactor due to gravity and assume that the chinstrap slows the impactor with a roughly constant deceleration, we can predict the following sequence in table 5. Note that the 'Before' values of the impact mass are the 'After' values from the previous impact while the 'Before' platform velocity is twice the impact mass velocity minus the previous 'After' platform velocity. The transition from 'Before' to 'After' is governed by the equations given above.

Although this analysis of the impact series is highly simplified, it captures much of the essence of the interaction. The impactor strikes the platform driving it downward. As the platform moves, it is retarded by the chinstraps until the moving impactor catches up and strikes it again and again and again. After six impacts, the calculation suggests that the impactor and platform are quickly approaching the point at which they will move together with the same velocity. The calculation also suggests that only half a Joule or so of the impact mass' original kinetic energy has been lost to heat and noise.

Table 5. B-95 Impact Interaction Sequence

B-95		Impact Mass		Platform Mass		
		Velocity	Energy	Velocity	Energy	Increment
1	Before	0.77 m/s	11.18 J	0	0	-

	After	0.71 m/s	9.51 J	1.13 m/s	1.28 J	1.28 J
2	Before	0.71 m/s	9.51 J	0.28 m/s	0.08 J	-
	After	0.67 m/s	8.64 J	0.91 m/s	0.83 J	0.75 J
3	Before	0.67 m/s	8.64 J	0.44 m/s	0.19 J	-
	After	0.66 m/s	8.18 J	0.79 m/s	0.62 J	0.43 J
4	Before	0.66 m/s	8.18 J	0.52 m/s	0.28 J	-
	After	0.65 m/s	7.92 J	0.72 m/s	0.52 J	0.24 J
5	Before	0.65 m/s	7.92 J	0.57 m/s	0.33 J	-
	After	0.64 m/s	7.78 J	0.68 m/s	0.46 J	0.14 J
6	Before	0.64 m/s	7.78 J	0.60 m/s	0.36 J	-
	After	0.64 m/s	7.71 J	0.66 m/s	0.43 J	0.08 J

The implications of this interaction is that the B-95 procedures stress the retention system with almost all the kinetic energy of the impact mass while the CPSC test may lose as much as half that energy to heat and noise. However, there is also another effect. Since gravity continues to act on all these masses throughout the interaction, their descent applies additional energy to the chinstraps as the platform descends. The pickup is as much as 2 additional Joules for the CPSC procedures and 9.8 Joules for B-95.

These calculations suggest that the CPSC test puts as much as 15 Joules into stressing the retention system and that B-95 applies as much as 21 Joules. Of course, the coefficient of restitution is a nominal value based on collisions of identical spheres and there is no allowance for friction and rotation as the impact mass drops in a guided fall to the platform. There will be energy losses before and during the impact. However, since we have collected time series data for the forces on the platform and its motion, we can attempt to calculate the work done on the platform and, consequently, the retention systems directly.

$$W_p = \int (F_p + F_b) dx_p \approx \sum ((F_{pm} + F_b)(x_{pm} - x_{p(n-1)}))$$

where:

$F_b$  is the bias in the force which is approximately equal to the preload

$F_p$  is the force measurement and  $x_p$  is the displacement

Subscript n refers to the nth element in the time series

The calculation yields an average value of 13.0 Joules for the CPSC tests on the helmet samples and 17.8 Joules for the Snell tests on identical samples. These values are independent of the theoretical speculations involved in the analysis of the energy transfer during impact. All that has been done is to integrate the product of the force versus displacement series up to the instant of peak dynamic deflection. Even so, the calculated work done on the chinstraps is consistent with the theoretical transfers of kinetic energy.

We performed three more series of tests with the simulated retention system: a CPSC series, a B-95 series and, finally, a B-90 series, essentially the B-95 test but with a drop of only 20 mm.

The results for all five series are shown in the following table.

Table 6. Results Summary - Five Test Series

	CPSC Helmets	CPSC Springs	B-95 Helmets	B-95 Springs	B-90 Springs
Nominal mgh	23.5 J	23.5 J	11.2 J	11.2 J	7.5 J
Peak Stretch	26.7 mm	23.9 mm	24.9 mm	27.7 mm	21.9 mm
Peak Force	202 lb	176 lb	264 lb	265 lb	229 lb
Total mgh	25.4 J	25.2 J	21.0 J	22.1 J	16.0 J
Ideal Transfer	15.0 J	14.8 J	20.5 J	21.6 J	15.6 J
Work	13.0 J	12.0 J	17.9 J	19.0 J	13.8 J

The 'Nominal mgh' is the calculated value of the kinetic energy of the impact mass just before it first strikes the platform. The peak stretch and force are the average values collected for the five test series. Total mgh is the total change in potential of the retention strength test mechanism when the retention system reaches its peak stretch. This is the upper limit of the energy that could be applied to the springs or to the retention system. The Ideal Transfer represents just how much of the Total mgh might actually be applied given the nominal coefficient of restitution of 5/9. Finally, the work is the integration of the force versus stretch measurements up to the instant when the peak stretch is attained.

The nominal mgh figures suggest that the CPSC test is much more severe than either of the Snell tests. Some of the disparity disappears when the change in potential arising from the displacement of the platform and impactor after the impact is added in but the CPSC test still seems markedly more severe than either B-95 or B-90. However, when the dynamics of the interaction between the impact mass and the platform are considered, B-90 appears slightly more demanding than CPSC and B-95 exceeds it considerably. The theoretical dynamics are confirmed by integrations of the force versus the deflection of the platform. The work values calculated are noticeably lower than the ideal energy transfer values but the differences can be ascribed to friction, and to the fact that the impacts are likely to be much less efficient than the collisions between identical perfect spheres suggested for the coefficient of restitution.

## Conclusions

This exercise indicates that, in terms of stress, both the B-95 and B-90 procedures for the dynamic strength of the retention system test are more severe than CPSC. The peak forces are greater and so is the actual work done in stretching the chinstraps. However, since the preload applied by CPSC is so much lower, the chinstraps may extend for as much as 7 millimeters before the chinstraps reach a state comparable to the initial state in the Snell tests. Since the maximum dynamic stretch criterion is the same for all three standards, a helmet could conceivably pass the Snell tests and still fail CPSC for excessive stretch.

The analysis also suggests that the coefficient of restitution plays a much stronger role in determining the loads applied in the CPSC procedures than in either the B-95 or B-90 procedures. Since this coefficient may depend on the dimensions of the impactor which is unspecified in the CPSC procedures there may well be appreciable variability in the stresses applied in CPSC retention strength testing performed at different laboratories.

It should be noted that for most currently available helmets, the retention strength test is not critical for either Snell or CPSC procedures. Helmets rarely fail because of excessive elongation and the plastics used in most buckles is either sufficiently tough for B-95 or will fracture at forces well below those of CPSC. For these reasons, helmets meeting the previous B-95 requirements should be accepted as qualifying to the CPSC standard. For the same reasons, the technical advantages of the Snell procedures and equipment do not justify the expense of any immediate change in the CPSC test procedures. The Snell Memorial Foundation has adopted the CPSC retention strength test for use in current Snell bicycle helmet certification programs.

### Acknowledgments

R.L. McCarty and E.H. Hunter performed all the testing and also suggested, designed and built the simulated retention system. Thanks also to W.G. Brown, J. Barnes and S.D. Johnson.

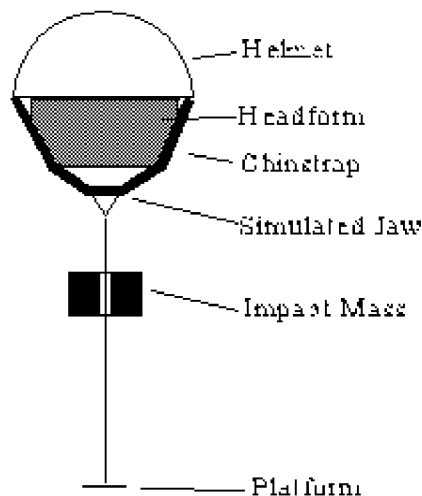
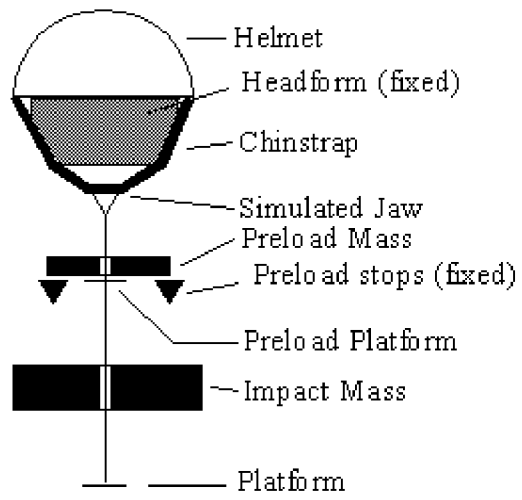


Figure 1 CPSC Test Device Schematic





**Figure 2** Snell Test Device Schematic

Supplementary est Results  
File # CA1 06/22/08

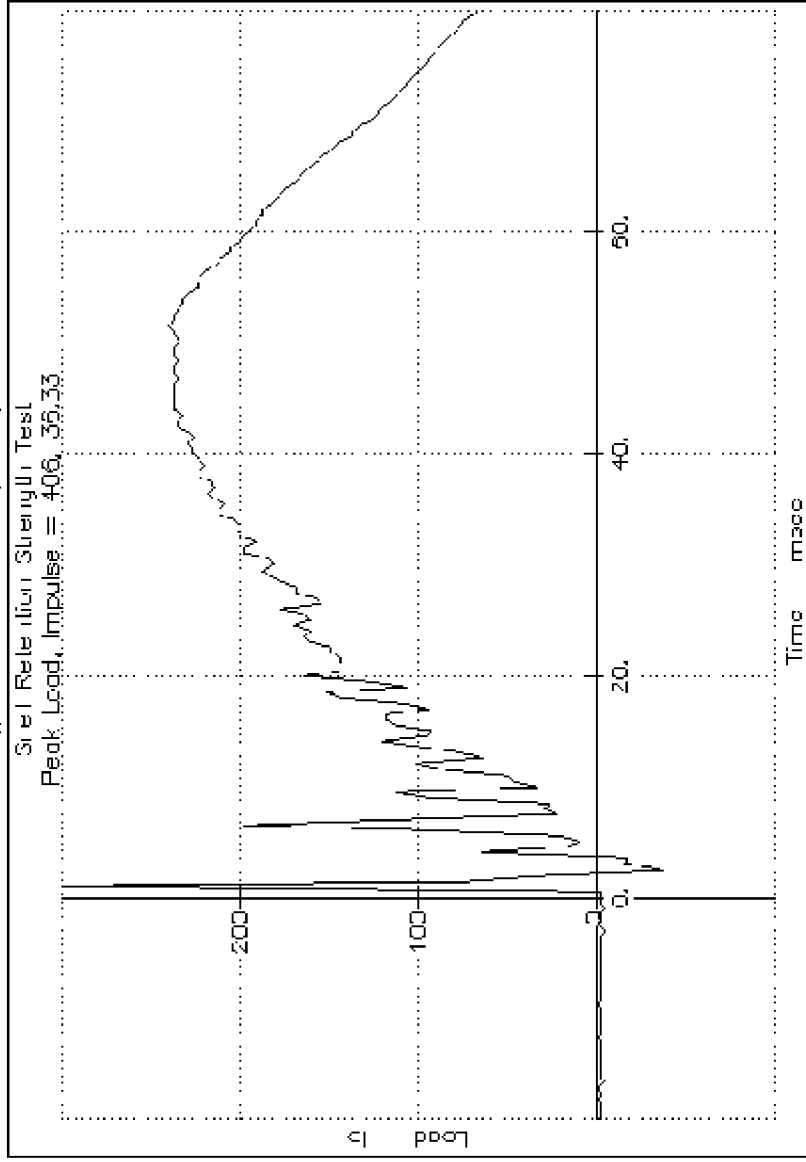


Figure 3 B-95 test Force versus Time

Supplementary est. Results  
File # CA1 06/22/98

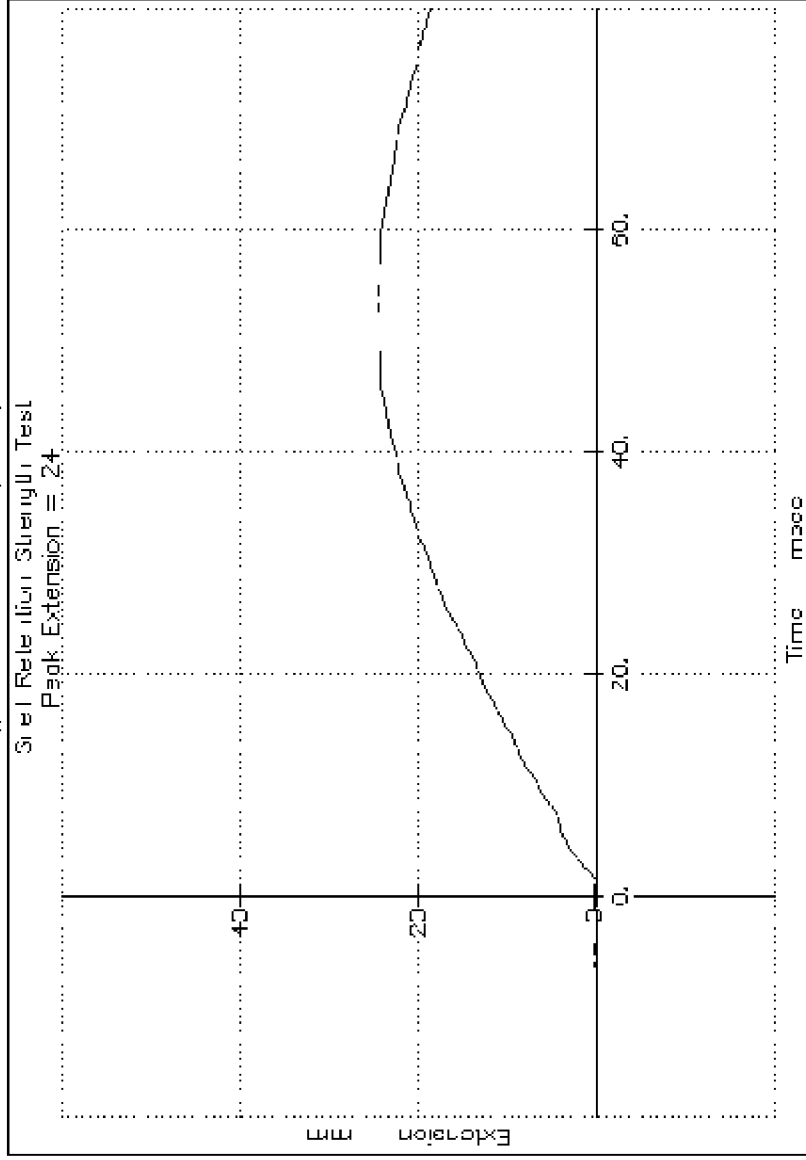


Figure 4 B-95 Test Displacement versus Time

Supplementary est. Results  
File # CA1 06/22/98

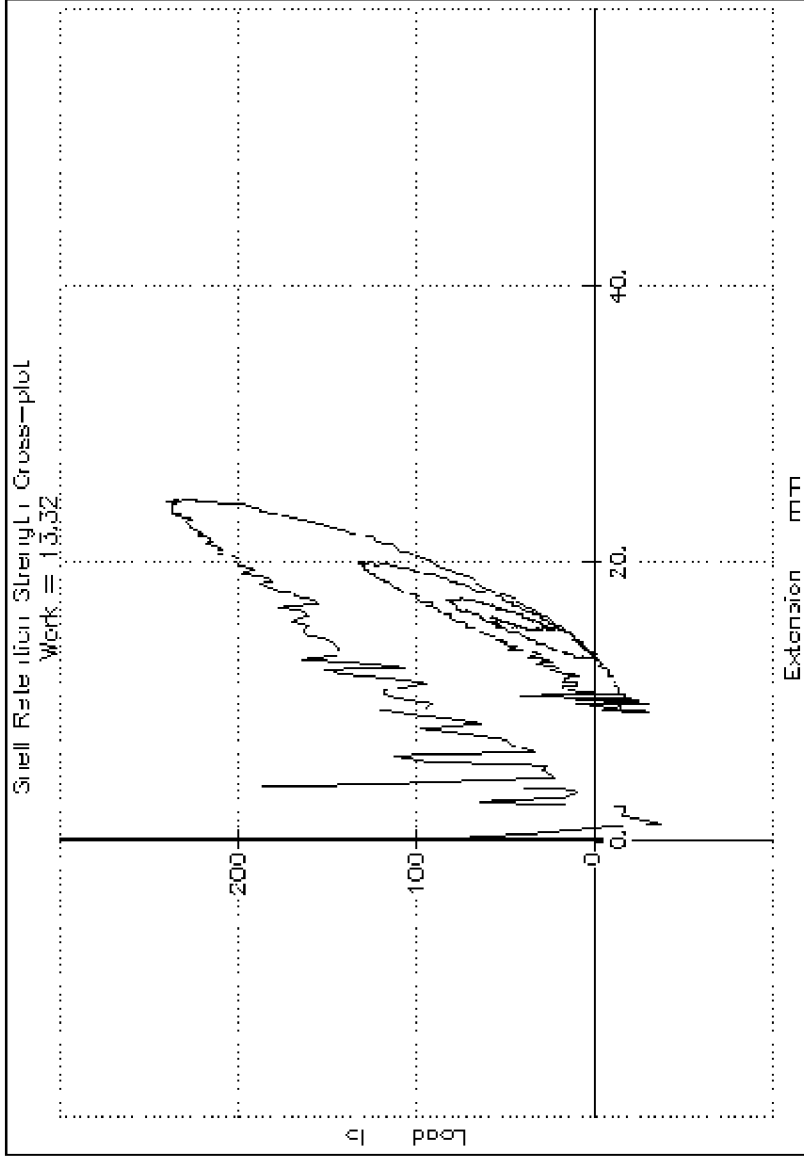


Figure 5 B-95 Test Force versus Displacement

Supplementary est. Results  
File # CA11 06/04/08

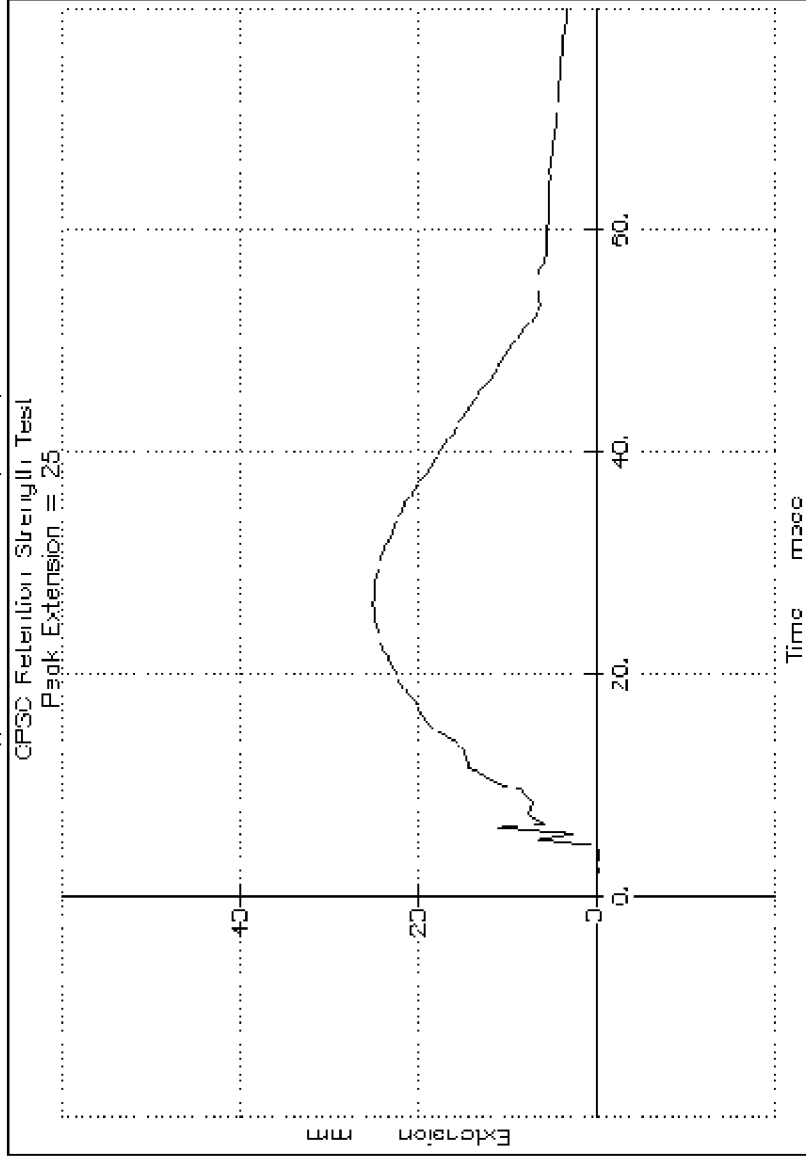


Figure 6 CPSC Test Displacement versus Time

Supplementary est Results  
File # CA11 06/04/08

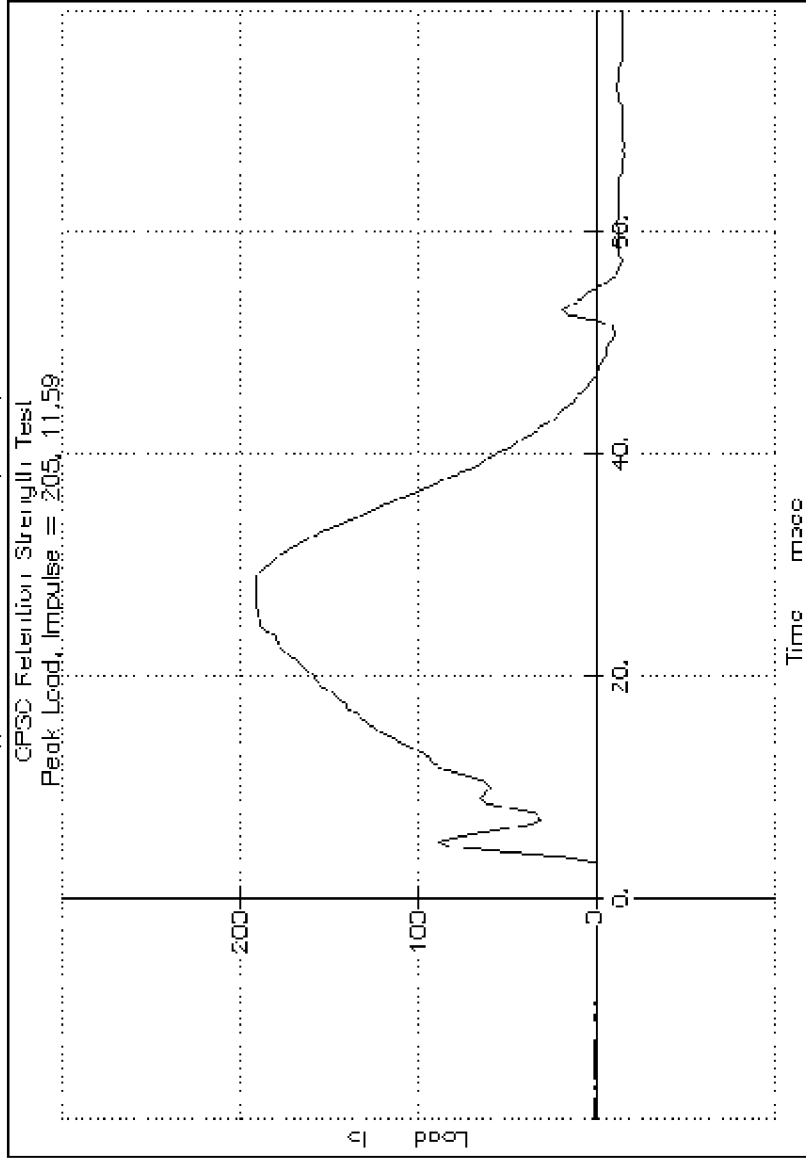


Figure 7 CPSC Test Force versus Time

Supplementary est. Results  
File # CA11 06/04/98

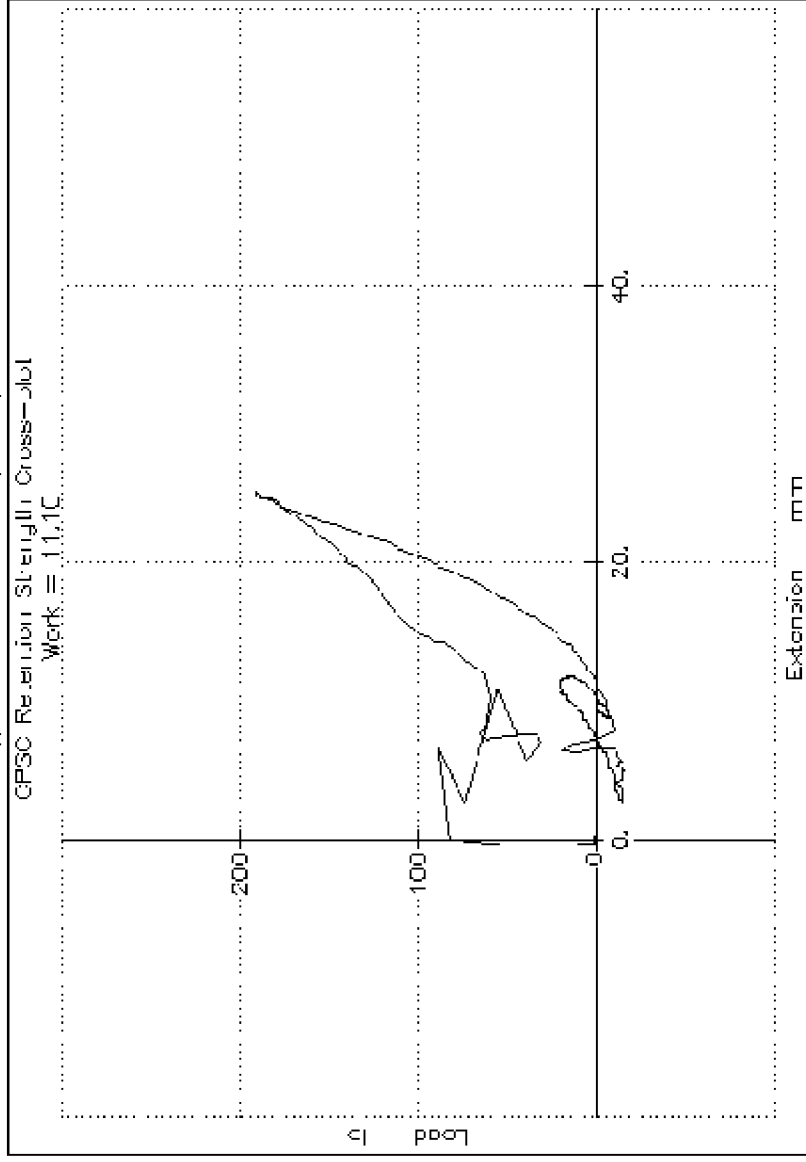


Figure 8 CPSC Test Force versus Displacement

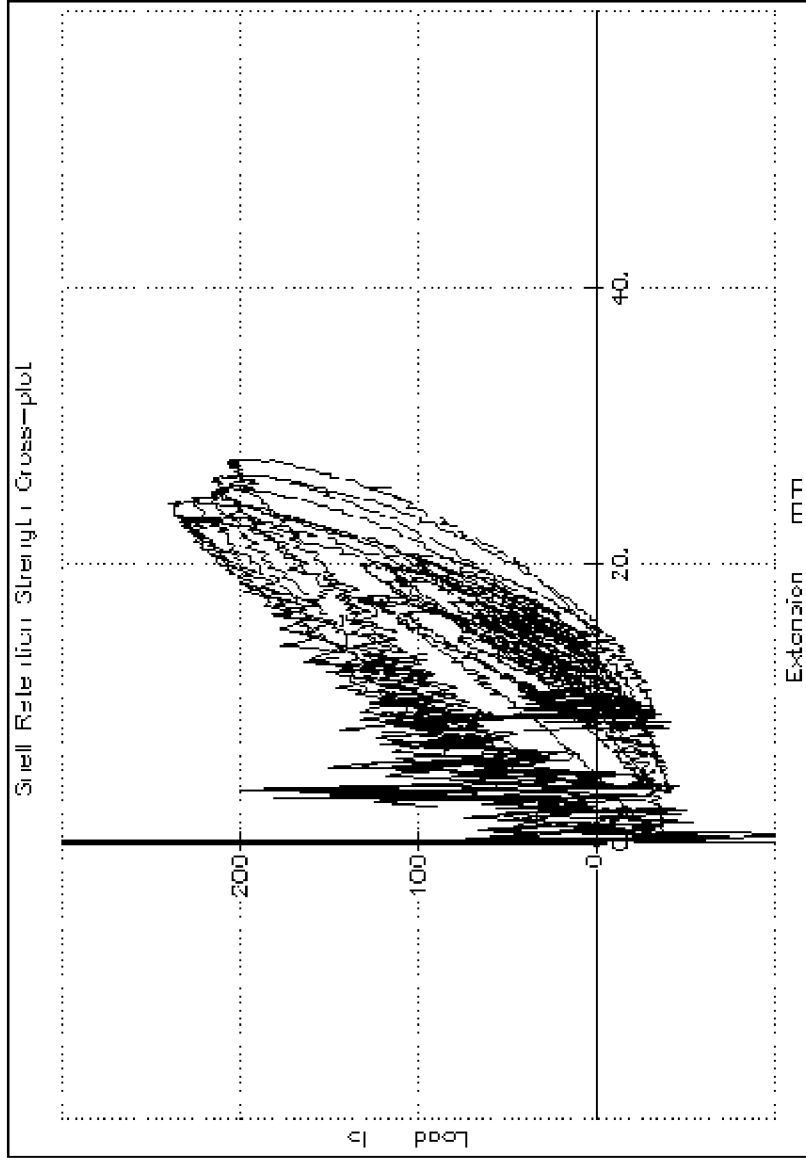


Figure 9 B-95 Force versus Displacement Traces



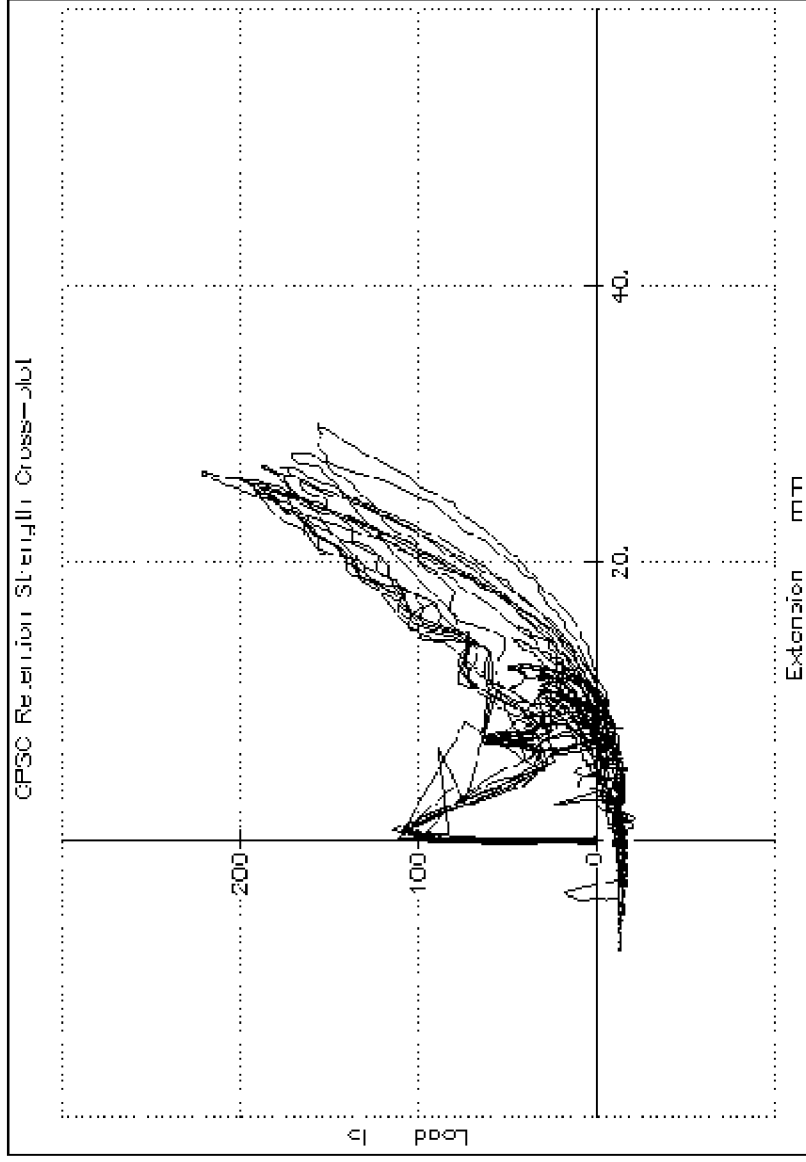


Figure 10 CPSC Force versus Displacement Traces

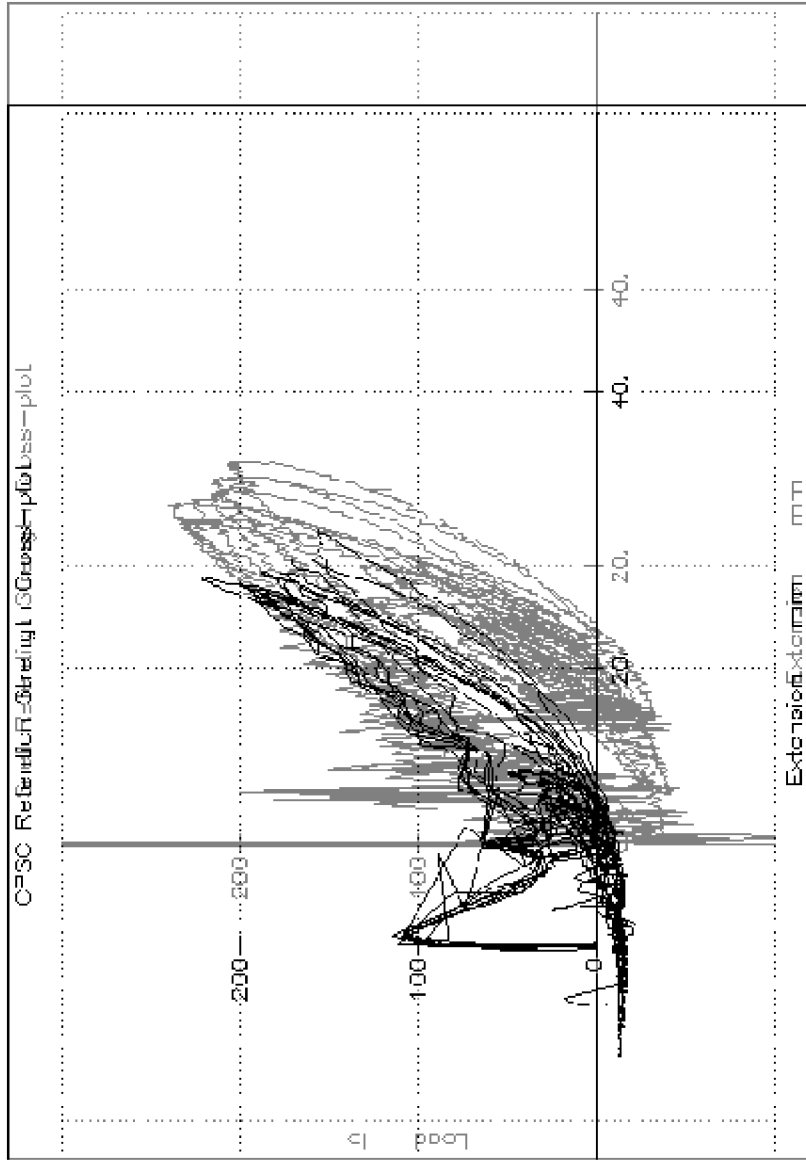


Figure 11 CPSC & B-95 Force versus Displacement Overlaid and Displacement Shifted